Published in final edited form as:
Cancer Biol Ther. 2009 December ; 8(24): 2406–2416.

Sorafenib inhibits ERK1/2 and MCL-1_L phosphorylation levels resulting in caspase-independent cell death in malignant pleural mesothelioma

Sharyn I. Katz[1,2,†], **Lanlan Zhou**[1,4,†], **Grace Chao**[2,4], **Charles D. Smith**[3], **Thomas Ferrara**[2], **Wenge Wang**[1], **David T. Dicker**[1], and **Wafik S. El-Deiry**[1,4,*]

[1]Laboratory of Molecular Oncology and Cell Cycle Regulation; Departments of Medicine (Hematology/Oncology); Genetics and Pharmacology; University of Pennsylvania School of Medicine; Philadelphia, PA USA

[2]Department of Radiology; University of Pennsylvania School of Medicine; Philadelphia, PA USA

[3]Medical University of South Carolina; Charleston, SC USA

[4]Bioengineering Graduate Group; the Institute for Translational Medicine and Therapeutics; and the Abramson Comprehensive Cancer Center; University of Pennsylvania School of Medicine; Philadelphia, PA USA

Abstract

Malignant pleural mesothelioma (MPM) is an aggressive, rapidly progressive malignancy without effective therapy. We evaluate sorafenib efficacy and impact on the cellular pro-survival machinery in vitro, efficacy of sorafenib as monotherapy and in combination with the naturally occurring death receptor agonist, TRAIL using human MPM cell lines, MSTO-211H, M30, REN, H28, H2052 and H2452. In vitro studies of the six MPM lines demonstrated single agent sensitivity to the multikinase inhibitor sorafenib and resistance to TRAIL. H28 and H2452 demonstrated augmented apoptosis with the addition of TRAIL to sorafenib in vitro. Treated cell lines demonstrated sorafenib-induced rapid dephosphorylation of AKT followed shortly by near complete dephosphorylation of the constitutively phosphorylated ERK1/2. Sorafenib therapy also decreased phosphorylation of B-Raf and mTOR in several cell lines. Within 3 h of sorafenib treatment, a number of known pro-survival molecules were dephosphorylated and/or downregulated in expression including MCL-1_L, c-$FLIP_L$, survivin and cIAP $_1$. These changes and eventual cell death did not elicit significant caspase-3 activation or PARP cleavage and pretreatment with the pan-caspase inhibitor, Z-VAD-FMK, did not block sorafenib efficacy but did block the effect of TRAIL monotherapy. Pre-treatment with Z-VAD-FMK did not block the synergistic effect of TRAIL and sorafenib in H28. In summary, single agent treatment with sorafenib results in widespread inhibition of the pro-survival machinery in vitro leading to cell death via a primarily caspase-independent mechanism. Combining sorafenib therapy with TRAIL, may be useful in order to provide a more efficient death signal and this synergistic effect appears to be caspase-independent. Pilot in vivo data demonstrates promising evidence of therapeutic efficacy in human tumor bearing xenograft *nu/nu* mice. We document single agent activity of sorafenib against MPM, unravel novel effects of sorafenib on anti-apoptotic signaling mediators, and suggest the combination of sorafenib plus TRAIL as possible therapy for clinical testing in MPM.

*Correspondence to: Wafik S. El-Deiry; wafik@mail.med.upenn.edu.
†These authors contributed equally to this work.

Keywords

mesothelioma; cancer therapy; cell death; sorafenib; MCL-1; imaging; TRAIL; caspase-independent

Introduction

Malignant pleural mesothelioma (MPM) is a rare but lethal malignancy of the pleura with nearly all afflicted succumbing to disease within 1 year of diagnosis.[1] While MPM is on the decline in the United States, a rise in cases is expected in Asia, Latin America and the Commonwealth of Independent States.2 In recent years pemetrexed, an antifolate metabolism drug, was added to therapy with cisplatin, a DNA damaging agent, and has become the standard of care for MPM, with only a marginal increase in survival over cisplatin alone.3,4 Improved, but modest, response rates have been achieved with combination therapy of cisplatin with gemcitabine, vinorelbine, ironotecan, raltitrexed or vinflunine. The resilient, aggressive nature of this malignancy is attributed to TRAIL resistance resulting from elevated baseline levels of known pro-survival effectors including $FLIP_L$,[5] HIF-1α,[6] $BCL\text{-}X_L$,[7,8] IAP-1,[9,10] survivin,[10,11] XIAP,[10] $MCL\text{-}1_L$, p21,12 PECAM-1,[13] HSP70 and the stem cell factor (SCF)/c-Kit/Slug pathway.[14] In addition to these resistance patterns, MPM human cell lines have also been demonstrated to have high levels of c-src15 and AKT pathway activity.

Tyrosine kinases are currently being explored primarily as inhibitors of VEGFR and EGFR signaling, both of which are highly expressed in MPM, and inhibitors of tumor proliferation via c-kit, PDGFR and ret. A novel tyrosine kinase inhibitor (TKI), sunitinib, is currently in clinical trials for potential response in mesothelioma.[16] To date, sorafenib therapy for MPM has only been reported in one patient in a Phase 1 trial of sorafenib in combination with doxorubicin.17 Sorafenib is generally well tolerated and has shown promise in a variety of malignancies including gastrointestinal malignancies, renal cell carcinoma, hepatocellular carcinoma and lung cancer. This drug inhibits PDGFR and VEGFR2 signaling and the Ras/Raf/MEK/ERK signaling pathway at the level of the serine/threonine kinase B-Raf and MEK.17 ERK1 and ERK2 have been demonstrated to have a pro-survival function resulting in stabilization of BCL family proteins including $MCL1_L$, and interference with pro-apoptotic BCL family members, such as the degradation of the proapoptotic Bim_{EL}.[18]

We explore the effects of treatment of sorafenib with or without TRAIL as chemotherapeutic agents for MPM in six human mesothelioma cell lines. The results document single agent activity of sorafenib against MPM, unravel novel effects of sorafenib on anti-apoptotic signaling mediators, and suggest the combination of sorafenib plus TRAIL as possible therapy for clinical testing in MPM.

Results

Human mesothelioma cell lines are sensitive to monotherapy with sorafenib in vitro

The highly motile human malignant pleural mesothelioma cell line, MSTO-211H, normally grows attached to the surface of the tissue culture wells assuming an elongated spindle-like appearance, maintaining intercellular attachments. Within 10 min of administration of sorafenib in vitro, MSTO-211H cells begin to undergo a rapid morphological change, including loss of attachment to each other and to the tissue culture plate surface assuming a more rounded appearance, which is followed within 15–20 min by the formation of surface irregularities in keeping with bleb formation suggestive of apoptosis (Fig. 1). However, western blotting of treated lysates of six human mesothelioma cell lines, MSTO-211H,

REN, H2452, H2052, H28 and M30 reveal little change in PARP cleavage products or cleaved activated caspase-3 (Fig. 2). Fluorescence activated cell sorting (FACS) analysis of MPM cell lines exposed for 9 h to sorafenib also failed to demonstrate significant activated caspase-3 by FACS analysis (Fig. 2). Sorafenib cell death was found to be dose-dependent both in short (10–24 h) (Fig. 2) and long exposures (32–38 hr) (data not shown) and was not inhibited by pre-treatment with the cell-permeant, irreversible, pan-caspase inhibitor Z-VAD-FMK.

Human MPM cell lines were TRAIL resistant with sorafenib-induced TRAIL sensitization

We tested whether the combination of sorafenib plus TRAIL may result in synergistic cell killing of MPM cell lines. In short and long-term cell killing assays, cells were treated with TRAIL, with or without pre-treatment with sorafenib in order to assess relative TRAIL resistance and possible sorafenib-induced TRAIL sensitization. As expected most cell lines, with the exception of MSTO-211H were relatively TRAIL resistant in short-term killing assays. In H2452 and H28, pre-treatment with low concentrations of sorafenib demonstrated a synergistic cytotoxic effect when followed by the addition of TRAIL (Fig. 2). Interestingly, this synergistic effect appears to be caspase-independent since it was not blocked by preincubation of cells with Z-VAD-FMK.

MPM cell line treatment with sorafenib rapidly induces dephosphorylation of AKT, ERK 1/2 and B-Raf

In order to further explore the signaling mechanism by which sorafenib results in cell killing, lysates from human MPM cells treated with sorafenib for varying time periods, (0, 15 min, 30 min, 1 h, 3 h) were analyzed for expression/phosphorylation status of positive and negative regulators of apoptosis and known targets of sorafenib. Interestingly, basal phosphorylation levels of VEGFR2 (tyrosines 951 & 1175), PDGFRβ were modest and revealed minimal changes after therapy with sorafenib in most cell lines (data not shown). Most of the cell lines demonstrated moderate levels of basal phosphorylation of B-Raf and C-Raf. With exposure to sorafenib, B-Raf was efficiently decreased in phosphorylation beginning at 15 min after initiation of therapy. Conversely, C-Raf, a weaker target of sorafenib, steadily increased in levels of phosphorylated C-Raf over a period of 15 min–3 h after exposure to sorafenib, but not TRAIL (Fig. 4).

With exposure to sorafenib, each cell line also revealed a moderate decrease in the phosphorylation levels of AKT which occurs by 15 min of exposure and recovers to near baseline phosphorylation levels by 1 h (Fig. 3). Temporally, this transient dephosphorylation of AKT was followed by a marked decrease in phosphorylation of ERK1/2 beginning at 30 min of exposure to sorafenib and remained suppressed, with unchanged levels of ERK1/2 total protein expression, and eventual near-recovery of baseline phosphorylation levels by 3 h (Fig. 3). These results suggest a transient dephosphorylation of AKT and ERK1/2 with recovery on the basis of an endogenous compensatory mechanism.

MPM cell line treatment with sorafenib induced rapid decreases in levels of anti-apoptotic proteins known to mediate resistance to death receptor signaling

Human malignant pleural mesothelioma cell line exposure to sorafenib resulted in early dramatic decreases in c-FLIP$_L$ (data not shown) and survivin levels with undetectable levels of the latter by 3 h. (Fig. 4). Interestingly, exposure to sorafenib, also resulted in an early steady decrease in the phosphorylation level of MCL-1$_L$ beginning at 15 min of sorafenib and undetectable levels of phopho-MCL-1 by 3 h. Initially stable, the levels of total MCL-1 protein began to decrease at 3 h of exposure to sorafenib (data not shown).

BCL_{XL} and Bim, pro-survival members of the BCL2 family, demonstrated constitutively very high levels with unchanged levels of bound Bax, Bid and PUMA after exposure to sorafenib as assessed by immunoprecipitation with BCL_{XL} and western blotting with antibodies to Bax, Bid and PUMA. BCL2 was not highly expressed in these cell lines. cIAP1, and to a lesser extent cIAP2, were expressed at low levels in most of the MPM cell lines and demonstrated a slight decrease in expression after exposure to sorafenib. XIAP was present in relatively high levels in one cell line, H2452, where there was no suppression of XIAP protein expression with sorafenib but there were boosted levels of XIAP protein with exposure to TRAIL, an effect previously observed with TRAIL therapy.

Finally, we assessed the pro-apoptotic mitochondrial proteins, Bax and Bid, which were expressed at high and modest levels respectively. These proteins were unchanged in protein expression levels with treatment with sorafenib (data not shown). Levels of cleaved caspase-3 demonstrated little change and PARP cleavage products only slightly increased after therapy with sorafenib.

Sorafenib-mediated cell death is independent of caspase activation

All six human MPM cell lines demonstrated very little caspase activation or PARP cleavage following sorafenib therapy which was assessed by western blotting of lysates obtained after up to 6 h after the addition of sorafenib. Caspase-3 activation was also assessed by FACS following 9 h of incubation with sorafenib and compared to staining with propidium iodide for estimation of the fraction of cells with sub-G_1 DNA content. Similarly, sorafenib induced little caspase-3 activation as observed by FACS despite accumulation of sub-G_1 cells in response to sorafenib therapy. To further confirm that sorafenib cell killing in MPM cell lines is caspase independent, cells were treated for 2 h with Z-VAD-FMK (10 μM), a potent, cell permeable, irreversible, pan-caspase inhibitor, prior to treatment with TRAIL and/or sorafenib. Cell viability was assessed by short-term Coomassie blue-stained viability assay and propidium iodide FACS. In all cell lines, Z-VAD-FMK demonstrated no significant effect on sorafenib-mediated cell killing whereas the caspase inhibitor did potently inhibit the cytotoxicity of TRAIL in those cell lines sensitive to TRAIL. Interestingly in the H28 cell line, the synergy between TRAIL and sorafenib therapy was unaffected by Z-VAD-FMK incubation indicating that this synergy is also caspase independent in nature.

Pilot trial of in vivo sorafenib therapy for human malignant pleural mesothelioma tumor-bearing xenografted nude mice demonstrate evidence of potential therapeutic efficacy

In order to establish a tumor-bearing xenograft model for human malignant pleural mesothelioma, we tested the ability of H28, H2052, H2452 and MSTO-211H to form subcutaneous tumors. Of these cell lines, only MSTO-211H reliably formed subcutaneous tumors and demonstrated expected tumor growth kinetics (data not shown) subcutaneously. Given the overall limited success with subcutaneous engraftment, several mice were grafted intraperitoneally (IP) with MSTO-211H cells surface-labeled with a cell membrane fluorescent label, CellVue Maroon, to allow detection of cell mass post-engraftment. Growth of MSTO-211H was robust in the peritoneal compartment. Both subcutaneous and IP grafted MSTO-211H demonstrated dramatic tumor regression with the administration of daily IP sorafenib over 3 w of therapy. The major observed side effect of therapy was a skin rash that appeared after 2 w of daily therapy and rapidly progressed just prior to termination of the experiment.

In this pilot trial of sorafenib therapy in a xenograft model of human malignant pleural mesothelioma, preliminary evidence was observed for a significant response of MPM to sorafenib therapy. This response was most dramatic in the MSTO-211H grown IP (Fig. 5).

The treated mouse with intraperitoneal tumor had markedly less gross tumor burden and evidence of marked cell death on histology. The CellVue Maroon membrane fluorescence did successfully identify the xenograft tumor cell mass intraperitoneally (Fig. 5) although the best tumor signal was obtained with the subcutaneous grafts.

Discussion

Malignant pleural mesothelioma (MPM) has been observed to be generally TRAIL-resistant which is thought to be mediated by a number of known pro-survival small molecules frequently active in malignancy. Specifically, resistance to therapeutics has been attributed to a number of mechanisms including elevated levels of pro-survival BCL2 members BCL-X_L, BCL2, MCL-1 and IAP members including XIAP, cIAP1, cIAP2, survivin, caspase-8 activation inhibitor, $FLIP_L$, and protein folding chaperones, heat shock protein 70 and 90 (HSP70 and HSP 90). In addition, MPM has been demonstrated to have constitutively elevated levels of growth factor activity, PDGFR, VEGFR and EGFR resulting in increased phosphorylation levels of the PI3K/AKT pathway including constitutively elevated levels of phosphorylation of ERK1/2. In this paper, we demonstrate single agent efficacy of sorafenib, a mutikinase inhibitor and experimental chemotherapeutic, in malignant pleural mesothelioma, and that cell death mediated by this agent in MPM lines appears to be caspase-independent and may be synergistic with TRAIL in some MPM tumors.

In the six human mesothelioma cell lines tested, the therapeutic efficacy of sorafenib appears to be partly on the basis of downregulation of a number of the MPM apoptotic resistance mechanisms including suppression of survivin, $FLIP_L$, cIAP1 and MCL-1 protein levels as well as suppression of AKT and blockade of ERK1/2 phosphorylation, common pathways for a number of pro-survival growth signals. Pro-apoptotic BCL2 family members including Bim, Bax, truncated Bid (tBid) were unchanged in expression levels up to 24 h of exposure to sorafenib. Furthermore, constitutive phosphorylation levels of PDGFRβ, VEGFR2, flt-3 and C-Kit, known targets of sorafenib and growth signals for MPM, were little changed by sorafenib exposure when expressed. There was an expected marked decrease in b-raf phosphorylation, a well known target of sorafenib, which was accompanied by a compensatory increase in C-Raf phosphorylation.

The effect on MCL-1 appeared mediated through effective suppression of MCL-1 phosphorylation, via inhibition of ERK1/2 phosphorylation, which was observed as early as 15 min after exposure to sorafenib. Phosphorylation of MCL-1 at threonine 163, the conserved MAP kinase/ERK site located within the PEST region, slows MCL-1 protein turnover and has a stabilizing effect on the protein,[19] with dephosphorylation leading to ubiquitinylation and degradation of MCL-1 initiated by phosphorylation at a conserved glycogen synthase kinase-3 (GSK-3) phosphorylation site at serine S159,[20] and subsequent association with E3 ligase beta-TrCP.21 This destabilizing effect was demonstrated in our data by a pronounced dephosphorylation of MCL-1 with initially stable protein levels followed by decreased MCL-1 protein levels beginning at 3 h of exposure to sorafenib. In addition to post-translational effects on MCL-1, decreases in MCL-1 protein levels may be also be the result of decreased transcription since MCL-1 is rapidly transcribed in response to growth factor stimulation via the PI3K/AKT pathway.

MCL-1 plays a prominent role in the inhibition of apoptosis, mediating its effects primarily through interaction with pro-apoptotic members of the BCL-2 family at the level of the mitochondria. MCL-1, which has rapid protein turnover, and BCL-X_L, which is relatively stable in expression and regulated through BH2 and BH3 domains, have been shown to bind to Bak[22] and Bax[23] and Bim_{EL}. BIM_{EL} is thought to play a pro-apoptotic role by blocking binding of Bax and Bak to BCL-X_L and MCL-1, thus freeing them to induce apoptosis.

Recently it has been shown that the Bim_{EL}/Mcl-1 and Bim_{EL}/BCL-X_L complexes can be rapidly dissociated following activation of ERK1/2 by survival factors thus allowing Bax and Bak binding to MCL-1 and BCL-X_L and thus inhibiting apoptosis.[23] Similarly, proapoptotic tBid migrates to the mitochondria following cleavage and activation by death receptor pathway initiator caspase 8, and binds tightly to MCL-1, displacing Bax and Bak and allowing them to oligomerize and induce mitochondrial cytochrome *c* release and subsequent apoptosis.[24] Downregulation of MCL-1 has been demonstrated to lead to coupling of stress-induced transcription factor eIF2alpha phosphorylation to mitochondrial apoptosis initiation[25] thus enabling but not committing the cell to apoptosis.

BCL-X_L prevents apoptosis through heterodimerization with pro-apoptotic proteins, and stabilization of the mitochondrial membrane by maintaining metabolite exchange across the outer mitochondrial membrane by inhibiting VDAC closure.[26–28] One exception is the heterodimerization of BCL-2 family member Bad with BCL-X_L which leads to apoptosis, the association of which is blocked by Bad phosphorylation and subsequent binding and sequestration by 14-3-3.[29] BCL-X_L has been demonstrated to inhibit caspases-3 and -9 and prevent nuclear translocation of apoptosis-inducing factor (AIF).[30] BCL-X_L regulation is not entirely understood however, it has been demonstrated that in some cell lines phosphorylation of BCL-X_L at serine 62 by stress response Jun kinase opposes the anti-apoptotic function of BCL-X_L permitting cells to die by apoptosis[31] by inhibiting its ability to bind to Bax.[32] Also caspase-3/CPP32-like proteases have been observed to cleave BCL-X_L protein resulting in accelerated apoptotic cell death.[33] In our studies of six MPM cell lines, all cell lines expressed very high levels of Bim and BCL-X_L and modest levels of Bax and Bid that were unchanged with treatment by sorafenib.

All six MPM cell lines expressed IAP pro-survival protein, survivin, which was suppressed but not eliminated in response to sorafenib therapy in vitro. Survivin is known to bind and inhibit caspase-3, controlling the checkpoint in the G_2/M-phase of the cell cycle through inhibiting apoptosis and promoting cell division. Another IAP member, XIAP, was expressed in one cell line, H2452, and was efficiently unchanged in expression after exposure with sorafenib. Consistent with previous literature, XIAP was noted to increase with treatment with TRAIL.

$FLIP_L$ expression levels were noted to be elevated in H2052, MSTO-211H, H2452 and M30 but not H28 and REN. In those cell lines with constitutively elevated $FLIP_L$, $FLIP_L$ levels were decreased but not completely suppressed by treatment with sorafenib. Furthermore, death-receptor signaling was found to be defective more proximally with relatively low levels of DR4 expression and low to absent levels of DR5 expression. Examination of caspase-3 activation revealed a lack of caspase-activation in all six cell lines after exposure to sorafenib which was confirmed by western blot analysis and FACS staining for activated caspase-3 despite efficient cell death by bright-field microscopy, cell-killing assays and propidium-iodide FACS analysis. Also deficient was the production of PARP cleavage products with treatment with sorafenib. These findings point to a caspase-independent cell death possibly through ER-stress, previously described for sorafenib, or apoptosis-inducing factor translocation to the nucleus.

These findings together with the initial in vivo therapeutic effects of sorafenib in our pilot trial of sorafenib in human MPM-tumor bearing mice, support a potential role for sorafenib in the therapy of malignant pleural mesothelioma. Sorafenib is currently being explored as a chemotherapeutic in clinical trials for a number malignancies including non-small lung cancer, breast cancer, renal cell carcinoma and bladder, colon, esophageal, hepatocellular, squamous cell and pancreatic cancer. To date with reference to sorafenib only one patient with malignant pleural mesothelioma is reported in the literature, and that patient was

reported to have had a partial response to combination therapy of doxirubicin with sorafenib[17] and remained on therapy for early 40 w. While sorafenib has notable toxicities including a rash, diarrhea and sensory deficits, perhaps in combination with other chemotherapeutics, doses can be lowered while still achieving efficacy as demonstrated in vitro in these six human cell lines. The combination of TRAIL or TRAIL receptor agonists plus sorafenib also holds promise and merits clinical testing in MPM.

Materials and Methods

Cell lines and cell culture

Human cell lines utilized for in vitro include MSTO-211H, H2052, H2452, H28 (purchased from ATCC) and REN, M30 (provided by Dr. Steven Albelda, University of Pennsylvania). Care was taken to limit the number of passages to less than 20 to avoid inadvertent in vitro selection. When not in use, cells were stored in liquid nitrogen in 10% DMSO/90% culture medium.

Cells were maintained in a humidified sterile environment with 5% CO_2, 37°C cultured in RPMI medium supplemented with 10% heat-inactivated fetal calf serum with 1% penicillin and streptomycin (CM). Passage of cell lines was performed at 1:5 dilution after detachment using sterile Gibco 0.5% Trypsin-EDTA solution (Invitrogen).

Bright field microscopy

Human mesothelioma cell line MSTO-211H was seeded into sterile 6-well tissue culture plates at a concentration of 0.6×10^6/mL in CM. Cells were allowed to adhere to the surface of the tissue culture plate by incubating at 5% CO_2, 37°C for 16–24 h. Sorafenib diluted in CM from 32 mM stock in DMSO, stored at −20°C or DMSO control was then added to designated wells and allowed to incubate overnight. After sorafenib incubation, TRAIL diluted in CM from a 1 mg/mL stock in dPBS stored at −20°C was added to designated wells for 2 h and the tissue culture plates loaded into a CO_2, temperature and humidity controlled tissue culture chamber attached to a bright-field microscope.

Short-term in vitro cell death assays

Cells were harvested from culture with 0.5% trypsin-EDTA and washed with the CM then plated at 0.6×10^6/well in a sterile 6-well tissue culture plate. Cells were then incubated at 37°C, 5% CO_2 for 18–24 h to allow attachment of cells to floor of the well. Sorafenib diluted in CM from 32 mM stock in DMSO, stored at −20°C was then added to the appropriate wells for a total of 4 mL CM and cells were allowed to incubated with sorafenib for 16–22 hr. For comparison, cells were also treated for 4 h of TRAIL therapy with and without pre-incubation with sorafenib, Flag-TRAIL diluted in CM from a 1 mg/mL stock was added to the appropriate wells at either 50 ng/mL or 100 ng/mL. Culture medium for wells, not containing sorafenib was treated with 0.1% DMSO to control for the possible effects of DMSO on the cell viability. Incubations with cell permeant irreversible, pan-caspase inhibitor Z-VAD-FMK [carbobenzoxy-valyl-alanyl-aspartyl-(O-methyl)-fluoromethylketone] (Promega) were performed by adding the purchased 20 mM Z-VAD-FMK/DMSO solution at a final concentration of 10 μM at 5% CO_2, 37°C, in a sterile humidified incubator for 2 h prior to addition of chemotherapy. After treatment, floating cells were presumed dead and aspirated. Adherent cells were washed with cold dPBS, fixed with 10% methanol/10% acetic acid solution for 10 min followed by 15 min staining with coomassie blue/methanol staining solution. Plates were then rinsed with distilled water and allowed to air-dry. Quantification of stained well optical density was performed with NIH Image J.

Long-term in vitro cell death assays

After incubations with treatments as detailed above in the “short-term cell killing assay,”, the cultures were allowed to incubate at 37°C, 5% CO_2 in th given chemotherapies for another 24 h at which point the cells were passaged. Floating cells, presumed dead, were aspirated and discarded. Adherent cells were washed with cold sterile dPBS then removed with 0.5% Trypsin-EDTA solution, and passaged in RPMI CM incubated at 37°C, 5% CO_2 for 72 h. Floating cells were again aspirated and adherent cells washed with cold dPBS, fixed with 10% methanol/10% acetic acid solution for 10 min followed by 15 min staining with Coomassie blue/methanol staining solution. Plates were then rinsed with distilled water and allowed to air-dry.

Propidium iodide FACS

After incubations with chemotherapies in a 60 mm tissue culture sterile petri dish, supernatants and adherent cells, using 0.5% Trypsin-EDTA, were removed from dish surface and washed with cold dPBS. Cell pellets were then resus-pended in 5 mL cold 75% ETOH and allowed to fix overnight-1 month at 4°C. On the day prior to FACS analysis, the ETOH was removed and cells were washed with cold dPBS. Cells were treated with 0.5 M phospho-citric acid buffer, then resuspended in a propidium iodide staining solution (RNase/PI in dPBS) and allowed to incubate overnight at 4°C. The cells were then analyzed by flow cytometry, the subG_1 fraction was measured.

Activated-caspase 3 FACS

Intracellular staining for activated caspase-3 was performed using the BD Pharmingen™ Caspase-3, Active Form Kit which is a mouse anti-human polyclonal anti-body conjugated with the fluorophore phycoerythrin (PE). After incubations with chemotherapeutic treatments, supernatants and adherent cells were both collected from the 6-well plates, using 0.5% Trypsin-EDTA, and washed with cold dPBS. Collected cells were fixed and permeabilized using the BD kit Fix/Perm™ solution. After incubation in the Fix/Perm™ solution for 24 hours-2 weeks at 4°C, cells were pelleted and washed twice with BD Perm/Wash™ buffer (1X) at a volume of 0.5 ml buffer/10^6 cells at room temperature. Cells were resuspended in BD Perm/Wash™ buffer (1X) plus antibody and incubated for 30 min at room temperature. Cells were then pelleted and washed in 1.0 ml BD Perm/Wash™ buffer (1X), then resuspended in 0.5 ml/sample in BD Perm/Wash™ buffer (1X) and analyzed by flow cytometry.

Western blotting

After cell culture and incubation with chemotherapy, cells adhered to the 6-well plates were removed with 0.5% Trypsin-EDTA and washed with cold dPBS. The supernatant was then aspirated and cells lysed with 800 μL 1x LDS Sample Buffer (*Invitrogen*, Carlsbad, CA) to which the reducing agent, 2-β-mercaptoethanol (2-ME), was added at a concentration of 6λ 2-ME/mL sample buffer. Cell lysates were transferred to 1.5 mL sterile Eppendorf tubes, vortexed, boiled at 100°C for 7 min, spun down to remove debris, and loaded on NuPAGE® Novex® Bis-Tris Gels 4–12% (Invitrogen). After electrophoresis, protein was transferred to a polyvinylidene fluoride (PVDF) membrane and non-specific binding blocked with a 5% non-fat milk buffer solution. Blots were then washed and probed with specific anti-human primary antibodies and developed using species specific horseradish-peroxidase (HRP)-conjugated secondary antibodies using enhanced chemiluminescence (ECL) with the Amersham™ *ECL* Plus *western blotting* Detection Reagents (GE Healthcare Biosciences, Pittsburg, PA). Primary and secondary antibodies were purchased from (C*ell Signaling*, Danvers, MA) with the exception of $FLIP_L$ (*Alexis Biochemicals*, Plymouth Meeting, PA),

DR4 (Imgenex) and survivin (Novus). Quantitation of gel band optical density was performed with NIH Image J.

Xenograft formation

Prior to the use of animal models for this pilot study of MPM xenograft feasibility, protocol approval was obtained by the IACUC at the University of Pennsylvania. Initially 3 mon old *nu/nu* female mice (Charles River laboratories) were injected subcutaneously in one flank with 2×10^6 cells suspended in a 50% sterile, endotoxin-free BD Matrigel™ (BD Biosciences, San Jose, CA) solution. This technique yielded poor xenograft tumor induction using H28 (one cage) and H2452 (one cage) with little tumor growth, and some tumor regression, over a 2 mon period. In order to optimize xenograft formation, a second tumor was induced in the contralateral thigh of mice from these cages and three additional cages were also inoculated each with a different MPM cell line in order to assess which if any human MPM cell line yielded quality xenograft formation.

Tumor xenografts were established by subcutaneous injection of 10^7 cells suspended in Ex vivo media (CellGro) and 50% BD Matrigel™ solution. Two mice from the cage of mice inoculated with MSTO-211H also was inoculated intraperitoneally with 10 million cells in Ex Vivo media (no Matrigel). The cells for these IP inoculations as well as the flank tumors from the MSTO-211H cage were coated with a fluorophore, CellVue® Maroon (Molecular Targeting Technologies, Inc., West Chester, PA), which inserts non-specifically into the lipid bilayer and allows tracking of the tumor with optical imaging. Once tumors were formed, a subset of each cage was treated with sorafenib 60 mg/Kg dissolved in a sterile Cremophor® EL solution (BASF Corporation, Florham Park, NJ) or vehicle (Cremophor® EL solution) IP daily for 3 w. During tumor induction and therapy, mice were housed in the five Richards Animal Facility at the University of Pennsylvania. After therapy/imaging completion, mice were humanely euthanized with ketamine i.p. followed by cervical dislocation in accordance with the IACUC regulations.

Histological analysis

After euthanasia, xenograft tumors were promptly excised, weighed and emerged into a 4% para-formaldehyde solution and allowed to incubate overnight at 4°C. The tissues were then removed and placed in a solution of 70% ethanol for 24 h-2 weeks, maintained at 4°C until paraffin embedding, performed at the GI Morphology Core, University of Pennsylvania, sectioned into 5 μm thick slices and mounted onto slides. Slides were stained in the Pathology Core, CHOP Stokes Research Facility.

References

1. Montanaro F, Rosato R, Gangemi M, et al. Survival of pleural malignant mesothelioma in Italy: a population-based study. Int J Cancer 2009;124:201–207. [PubMed: 18792097]
2. Kazan-Allen L. Asbestos and mesothelioma: worldwide trends. Lung Cancer 2005;49:3–8.
3. Goudar RK. Review of pemetrexed in combination with cisplatin for the treatment of malignant pleural mesothelioma. Ther Clin Risk Manag 2008;4:205–211. [PubMed: 18728709]
4. Kindler HL. Systemic treatments for mesothelioma: standard and novel. Curr Treat Options Oncol 2008;9:171–179. [PubMed: 18770046]
5. Rippo MR, Moretti S, Vescovi S, et al. FLIP overexpression inhibits death receptor-induced apoptosis in malignant mesothelial cells. Oncogene 2004;23:7753–7760. [PubMed: 15334061]
6. Riganti C, Doublier S, Aldieri E, et al. Asbestos induces doxorubicin resistance in MM98 mesothelioma cells via HIF-1alpha. Eur Respir J 2008;32:443–451. [PubMed: 18385176]

7. Smythe WR, Mohuiddin I, Ozveran M, Cao XX. Antisense therapy for malignant mesothelioma with oligonucleotides targeting the BCL-X_L gene product. J Thorac Cardiovasc Surg 2002;123:1191–1198. [PubMed: 12063468]
8. Hopkins-Donaldson S, Cathomas R, Simoes-Wust AP, et al. Induction of apoptosis and chemosensitization of mesothelioma cells by Bcl-2 and BCL-X_L antisense treatment. Int J Cancer 2003;106:160–166. [PubMed: 12800189]
9. Gordon GJ, Appasani K, Parcells JP, et al. Inhibitor of apoptosis protein-1 promotes tumor cell survival in mesothelioma. Carcinogenesis 2002;23:1017–1024. [PubMed: 12082024]
10. Zangemeister-Wittke U, Hopkins-Donaldson S. Apoptosis regulation and drug resistance in malignant pleural mesothelioma. Lung Cancer 2005;49:105–108.
11. Falleni M, Pellegrini C, Marchetti A, et al. Quantitative evaluation of the apoptosis regulating genes Survivin, Bcl-2 and Bax in inflammatory and malignant pleural lesions. Lung Cancer 2005;48:211–216. [PubMed: 15829320]
12. Lazzarini R, Moretti S, Orecchia S, Betta PG, Procopio A, Catalano A. Enhanced antitumor therapy by inhibition of $p21^{waf1}$ in human malignant mesothelioma. Clin Cancer Res 2008;14:5099–5107. [PubMed: 18698027]
13. Bergom C, Goel R, Paddock C, et al. The cell-adhesion and signaling molecule PECAM-1 is a molecular mediator of resistance to genotoxic chemotherapy. Cancer Biol Ther 2006;5:1699–1707. [PubMed: 17106245]
14. Catalano A, Rodilossi S, Rippo MR, Caprari P, Procopio A. Induction of stem cell factor/c-Kit/slug signal transduction in multidrug-resistant malignant mesothelioma cells. J Biol Chem 2004;279:46706–46714. [PubMed: 15337769]
15. Tsao AS, He D, Saigal B, et al. Inhibition of c-Src expression and activation in malignant pleural mesothelioma tissues leads to apoptosis, cell cycle arrest, and decreased migration and invasion. Mol Cancer Ther 2007;6:1962–1972. [PubMed: 17620427]
16. Buckstein R, Meyer RM, Seymour L, et al. Phase II testing of sunitinib: the National Cancer Institute of Canada Clinical Trials Group IND Program Trials IND.182-5. Curr Oncol 2007;14:154–161. [PubMed: 17710208]
17. Richly H, Henning BF, Kupsch P, et al. Results of a Phase I trial of sorafenib (BAY 43-9006) in combination with doxorubicin in patients with refractory solid tumors. Ann Oncol 2006;17:866–873. [PubMed: 16500908]
18. Balmanno K, Cook SJ. Tumour cell survival signalling by the ERK1/2 pathway. Cell Death Differ 2009;16:368–377. [PubMed: 18846109]
19. Domina AM, Vrana JA, Gregory MA, Hann SR, Craig RW. MCL1 is phosphorylated in the PEST region and stabilized upon ERK activation in viable cells, and at additional sites with cytotoxic okadaic acid or taxol. Oncogene 2004;23:5301–5315. [PubMed: 15241487]
20. Maurer U, Charvet C, Wagman AS, Dejardin E, Green DR. Glycogen synthase kinase-3 regulates mitochondrial outer membrane permeabilization and apoptosis by destabilization of MCL-1. Mol Cell 2006;21:749–760. [PubMed: 16543145]
21. Ding Q, He X, Hsu JM, et al. Degradation of Mcl-1 by beta-TrCP mediates glycogen synthase kinase 3-induced tumor suppression and chemosensitization. Mol Cell Biol 2007;27:4006–4017. [PubMed: 17387146]
22. Pearce AF, Lyles DS. Vesicular stomatitis virus induces apoptosis primarily through Bak rather than Bax by inactivating Mcl-1 and BCL-X_L. J Virol 2009;83:9102–9112. [PubMed: 19587033]
23. Ewings KE, Hadfield-Moorhouse K, Wiggins CM, et al. ERK1/2-dependent phosphorylation of Bim_{EL} promotes its rapid dissociation from Mcl-1 and BCL-X_L. EMBO J 2007;26:2856–2867. [PubMed: 17525735]
24. Clohessy JG, Zhuang J, de Boer J, Gil-Gomez G, Brady HJ. Mcl-1 interacts with truncated Bid and inhibits its induction of cytochrome *c* release and its role in receptor-mediated apoptosis. J Biol Chem 2006;281:5750–5759. [PubMed: 16380381]
25. Fritsch RM, Schneider G, Saur D, Scheibel M, Schmid RM. Translational repression of MCL-1 couples stress-induced eIF2alpha phosphorylation to mitochondrial apoptosis initiation. J Biol Chem 2007;282:22551–22562. [PubMed: 17553788]

26. Minn AJ, Kettlun CS, Liang H, et al. BCL-X_L regulates apoptosis by heterodimerization-dependent and -independent mechanisms. EMBO J 1999;18:632–643. [PubMed: 9927423]
27. Vander Heiden MG, Li XX, Gottleib E, Hill RB, Thompson CB, Colombini M. BCL-X_L promotes the open configuration of the voltage-dependent anion channel and metabolite passage through the outer mitochondrial membrane. J Biol Chem 2001;276:19414–19419. [PubMed: 11259441]
28. Lama D, Sankararamakrishnan R. Anti-apoptotic BCL-X_L protein in complex with BH3 peptides of pro-apoptotic Bak, Bad and Bim proteins: comparative molecular dynamics simulations. Proteins 2008;73:492–514. [PubMed: 18452209]
29. Tan Y, Demeter MR, Ruan H, Comb MJ. BAD Ser-155 phosphorylation regulates BAD/BCL-X_L interaction and cell survival. J Biol Chem 2000;275:25865–25869. [PubMed: 10837486]
30. Yin W, Cao G, Johnnides MJ, et al. TAT-mediated delivery of BCL-X_L protein is neuroprotective against neonatal hypoxic-ischemic brain injury via inhibition of caspases and AIF. Neurobiol Dis 2006;21:358–371. [PubMed: 16140540]
31. Basu A, Haldar S. Identification of a novel BCL-X_L phosphorylation site regulating the sensitivity of taxolor 2-methoxyestradiol-induced apoptosis. FEBS Lett 2003;538:41–47. [PubMed: 12633850]
32. Upreti M, Galitovskaya EN, Chu R, et al. Identification of the major phosphorylation site in BCL-X_L induced by microtubule inhibitors and analysis of its functional significance. J Biol Chem 2008;283:35517–35525. [PubMed: 18974096]
33. Fujita N, Nagahashi A, Nagashima K, Rokudai S, Tsuruo T. Acceleration of apoptotic cell death after the cleavage of BCL-X_L protein by caspase-3-like proteases. Oncogene 1998;17:1295–1304. [PubMed: 9771973]

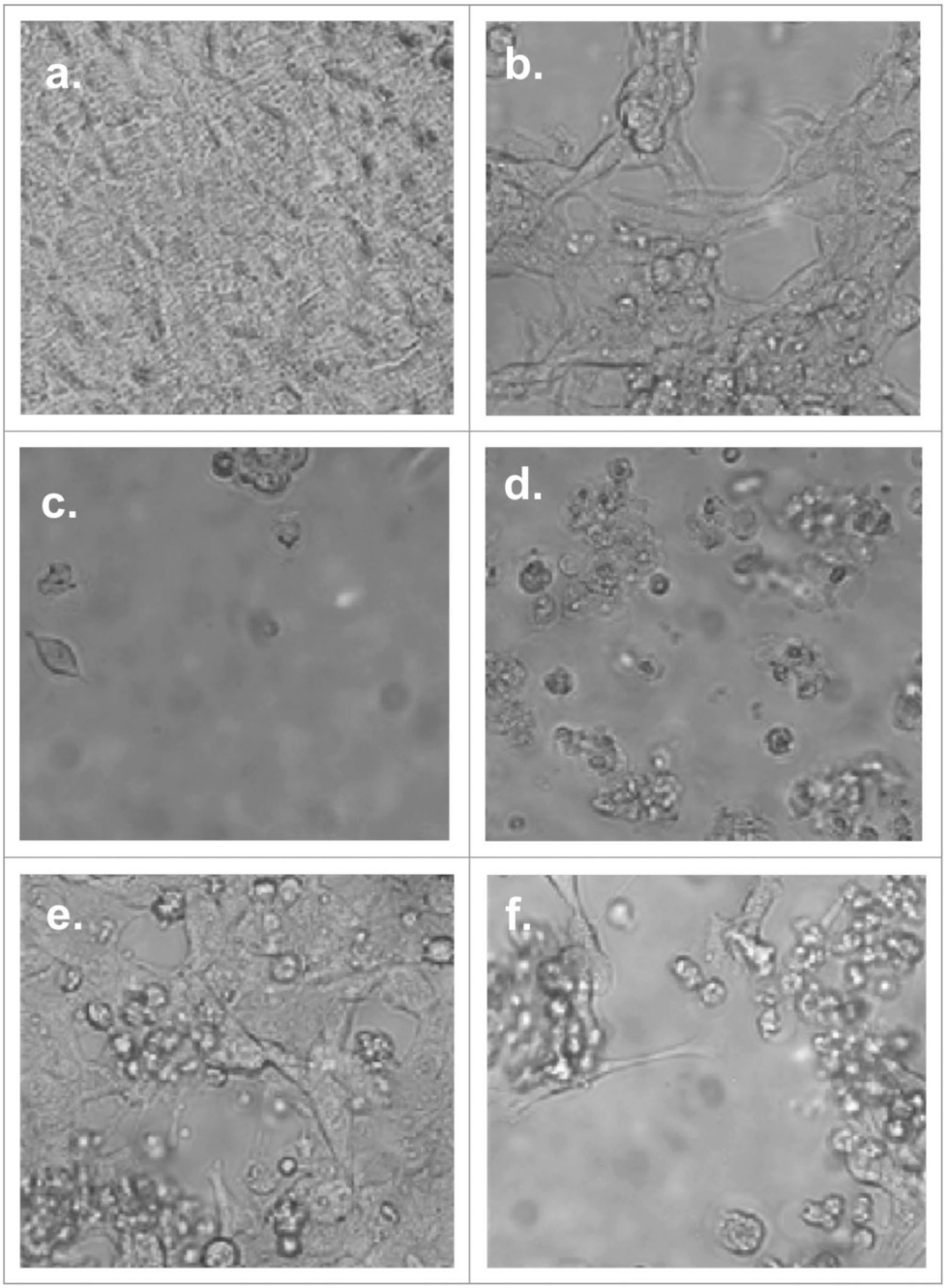

Figure 1.

Effects of incubation of MSTO-211H with TRAIL and sorafenib. Cells were allowed to adhere in sterile tissue culture plates for 16–24 h at 5% CO_2, 37°C. Sorafenib or vehicle (0.1% DMSO) were added to the plates and incubated for additional 16–22 h. TRAIL was added to designated wells and wells were then imaged with bright field microscopy. Chemotherapy assignment and concentrations are as follows: (a) control, (b) Sorafenib (16 μM), (c) Sorafenib (64 μM), (d) Sorafenib (64 μM) & TRAIL (100 ng/mL), (e) TRAIL (50 ng/mL) and (f) TRAIL (100 ng/mL). Images demonstrate a dose-dependent response of MSTO-211H to sorafenib and TRAIL with a marked sensitivity to sorafenib and to the combination of TRAIL and sorafenib.

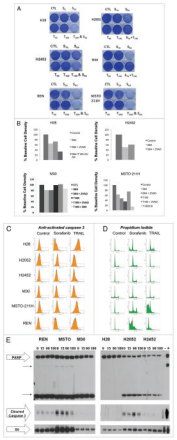

Figure 2.

In vitro exposure of MPM cell lines to sorafenib demonstrate cytotoxicity without significant induction of caspase-3 activation or PA RP cleavage products. All six MPM cell lines, REN, MSTO-211H, M30, H28, H2052 and H2452, were allowed 24 h to adhere to tissue culture plates. (A) Coomassie blue staining demonstrating the sensitivity profile of the six cell lines to TRAIL and sorafenib. (B) Coomassie blue staining of MPM cell lines with and without pre-treatment with the irreversible pan-caspase inhibitor, Z-VAD-FMK prior to sorafenib and/or TRAIL therapy. Immunoblotting was performed S6 loading control (bottom); cleaved caspase 3; PA RP (large arrow) and PA RP cleavage products (two smaller arrows) (Cell Signaling, Danvers, MA). Control lysate, purchased from *Cell Signaling*, Danvers, MA, for apoptosis were also added as the (−) and (+) lanes, representing Jurkat cells untreated or treated with etoposide respectively. (C) Anti-activated caspase FACS histograms of MPM cell lines treated with sorafenib or TRAIL, fixed and stained with PE-conjugated anti-activated caspase 3 antibody. (D) Propidium iodide FACS histogram of MPM cell lines treated with sorafenib or TRAIL, fixed and stained with propidium iodide. (E) Western blot analysis of MPM cell lysates following treatment with sorafenib 64 μM or vehicle (0.1% DMSO) for a 3 h time course. Immunoblotting was performed S6 loading control (bottom); cleaved caspase 3; PA RP (large arrow) and PARP cleavage products (two smaller arrows) (Cell Signaling, Danvers, MA). Control lysate, purchased from Cell Signaling, Danvers, MA, for apoptosis were also added as the (−) and (+) lanes, representing Jurkat cells untreated or treated with etoposide respectively.

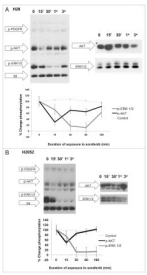

Figure 3.

Time course of treatment of human MPM cell lines with Sorafenib (64 μM) results in an early decrease in phosphorylation in AKT followed by a marked decrease in ERK 1/2 phosphorylation in whole cell lysates. In vitro cell cultures of H28 (A) and H2052 (B) were treated with sorafenib at a concentration of 64 μM at 37°C, 5% CO_2 for 0 (no sorafenib), 15 min (15'), 30 min (30'), 1 h (1°) and 3 h (3°). Cells were then washed with dPBS and lysed in 1X LDS sample buffer with 2-ME, boiled and run on a 4–12% pre-cast Nupage gel followed by immunoblotting with the following primary antibodies: PDGFR pathway activation antibody cocktail (Cell Signaling) with antibodies to phospho-PDGFR, phosphor-SHP 2, phospho-AKT, phosphor-ERK 1/2 and S6 loading control. These data reveal an early marked decrease in the phosphorylation levels of AKT in response to treatment with sorafenib with near recovery to baseline levels by 3 h of sorafenib exposure. This is followed temporally by a sharp, sustained dephosphorylation of ERK1/2 that begins to recover by 3 h of sorafenib therapy.

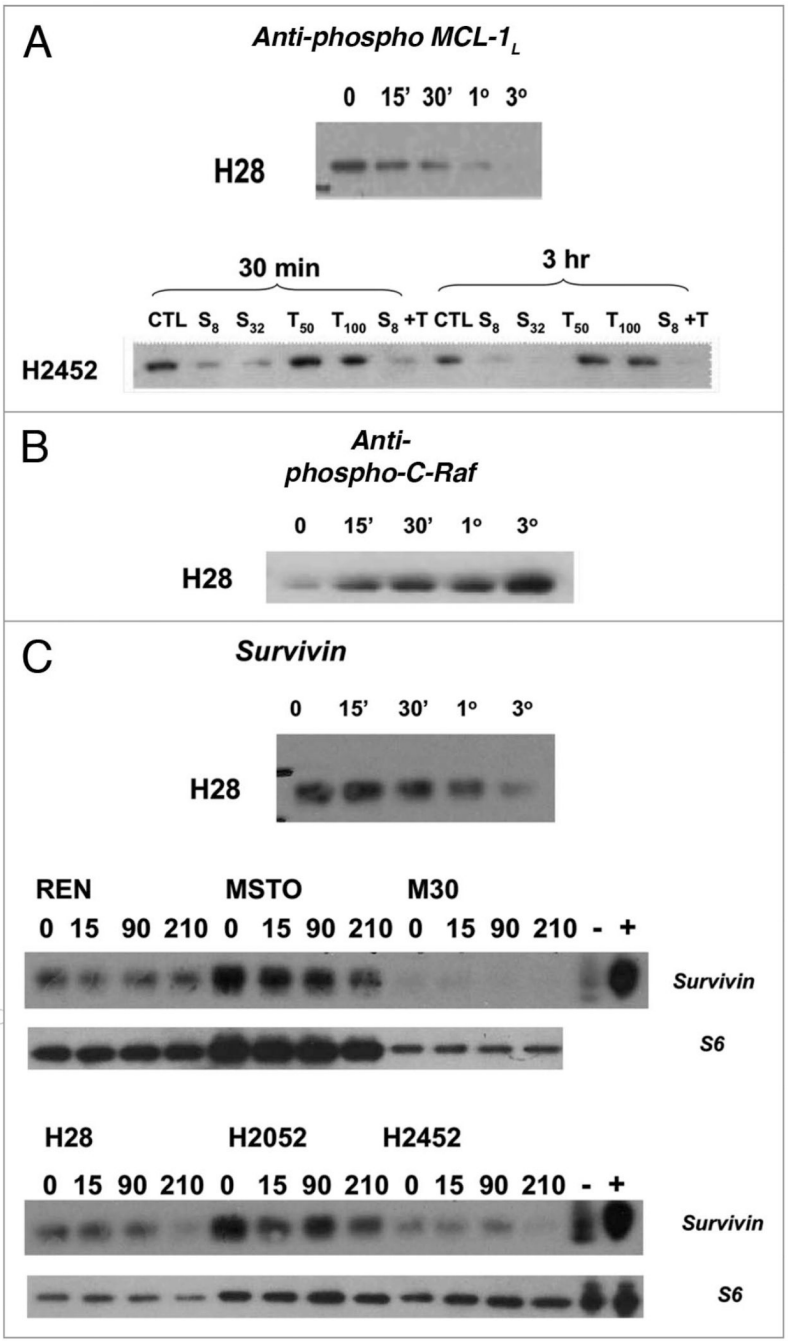

Figure 4.

Time course of treatment of human MPM cell lines with Sorafenib (64 μM) results in negative regulation of anti-apoptotic resistance proteins. *MPM* in vitro cell cultures were treated with sorafenib at a concentration of 64 μM at 37°C, 5% CO_2 for 0 (no sorafenib), 15 min (15'), 30 min (30'), 1 h (1°) and 3 h (3°). Cells were then washed with dPBS and lysed in 1X LDS sample buffer with 2-ME, boiled and run on a 4–12% pre-cast Nupage gel followed by immunoblotting with the following primary antibodies: (A) phospho-MCL-1_L (B) C-Raf (C) survivin (Cell Signaling). Sorafenib therapy resulted in dephosphorylation of MCL1 followed by decreased protein levels of MCL1 (data not shown) and decreased protein levels of survivin.

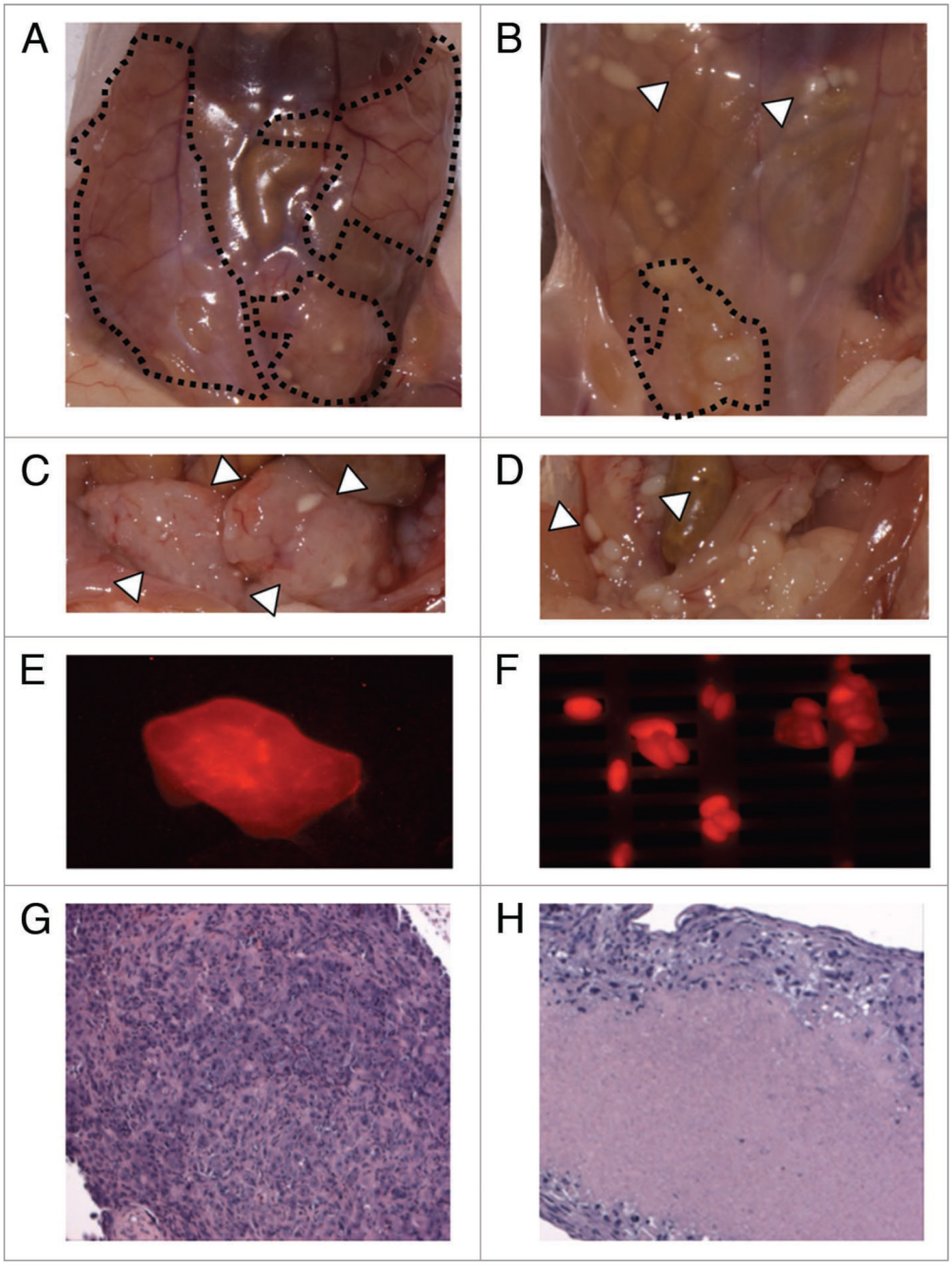

Figure 5.

Pilot evaluation of human MPM cell lines in a xenograft mouse models suggests sorafenib efficacy. *nu/nu* mice were injected IP with human malignant pleural mesothelioma cell line, MSTO-211H cell surface labeled with a fluorescent label, CellVue Maroon. Images above demonstrate (A) untreated (3 w daily IP vehicle) (B) treated with sorafenib 60 mg/Kg daily for 3 w (C) exposed untreated tumor with peritoneum resected (D) exposed treated tumor with peritoneum resected (E) large soft tissue IP tumors (F) and smaller tumor lesions demonstrate fluorescence in the expected excitation/absorption spectrum for CellVue Maroon cell surface labeled MSTO-211H utilized for these IP injected tumors. Immediately after sacrifice, xenografted tumor tissues were dissected, fixed in 4% formalin, paraffin-

embedded, sectioned in 6 μm slices and stained with hematoxylin and eosin. Treated tumor nodules demonstrated marked hyalinization and reduce tumor viability (H) compared with untreated tumor (G).